Available online at www.sciencedirect.com

ScienceDirect

journal homepage: www.elsevier.com/locate/watres

Increased nitrous oxide accumulation by bioelectrochemical denitrification under autotrophic conditions: Kinetics and expression of denitrification pathway genes

Tuan Van Doan [a,1], Tae Kwon Lee [a,1], Sudheer Kumar Shukla [a], James M. Tiedje [a,b], Joonhong Park [a,*]

[a] School of Civil and Environmental Engineering, Yonsei University, Seoul 120-749, Republic of Korea
[b] Center for Microbial Ecology, Michigan State University, East Lansing, MI 48824, USA

ARTICLE INFO

Article history:
Received 5 April 2013
Received in revised form
7 August 2013
Accepted 27 August 2013
Available online 23 October 2013

Keywords:
Bioelectrochemical system
Biocathode denitrification
Microbial fuel cell
Pyrosequencing

ABSTRACT

Under autotrophic conditions, we investigated the effects of different current densities on bioelectrochemical denitrification (BED). In this study, nitrate consumption and nitrous oxide (N_2O) production, microbial diversity and population dynamics, and denitrification pathway gene expressions were explored in continuous flow BED reactors at different current densities (0.2, 1, 5, 10 and 20 A/m^2). We found that, under the autotrophic conditions, N_2O accumulation was increased with increase in current density. The maximum rate of denitrification was 1.65 NO_3^-–N (g/NCCm^3.h), and approximately 70% of the reduced N was accumulated as N_2O. After each current density was applied, pyrosequencing of the expressed 16S rRNA genes amplified from the cathodic biofilms revealed that that 16 genera were active and in common at all currents, and that eight of those showed a statistically significant correlation with particular current densities. The relative expression of *napA* and *narG* was highest, whereas *nosZ* was low relative to its level in the inoculum suggesting that this could have contributed the high N_2O accumulation. Kinetic analysis of nitrate reduction and N_2O accumulation followed Michaelis–Menten kinetics. The V_{max} for nitrate consumption and N_2O accumulation were similar, however the K_m values determined as A/m^2 were not. This study provides better understanding of the community and kinetics of a current-fed, autotrophic, cathodic biofilm for evaluating its potential for scale-up and for N_2O recovery.

1. Introduction

The combination of microbiology and electrochemistry is a promising technology that uses microbial catalysis to drive electrochemical processes, known as bioelectrochemical systems (BESs). This emerging technology is applicable in wastewater treatment because of its unique capability of converting the chemical energy of organic waste, including

* *Corresponding author*. Tel.: +82 2 2123 5798; fax: +82 2 312 5798.
E-mail address: parkj@yonsei.ac.kr (J. Park).

[1] The two authors are equally contributed to this study as the first authors.

0043-1354/$ – see front matter © 2013 Elsevier Ltd. All rights reserved.
http://dx.doi.org/10.1016/j.watres.2013.08.041

low-strength wastewaters and lignocellulosic biomass, into electricity, hydrogen or chemical products (Pant et al., 2012; Rabaey and Verstraete, 2005; Logan et al., 2006), and/or of driving bio-reduction of inorganic and organic oxidized pollutants such as nitrate and tetrachloroethene (Clauwaert et al., 2007; Cheng et al., 2012).

For over 50 years heterotrophic driven denitrifying processes have been used in treating nitrate from wastewater. The disadvantages of the current heterotrophic denitrification are extra-cost for the addition of extracellular organic carbon (EOC) source(s) such as methanol, reactor clogging and excessive sludge production due to fast growth of denitrifying heterotrophs (Ghafari et al., 2008). Alternatively, microbial denitrification under the autotrophic conditions has been considered in treating nitrate from wastewater. Recent studies showed that autotrophic denitrification occurred in biocathode reactors (Clauwaert et al., 2007; Cheng et al., 2012; Puig et al., 2011; Virdis et al., 2008; Watanabe et al., 2001; Wang and Qu, 2003). Although the rate of nitrate removal via cathodic (autotrophic) denitrification is generally smaller than that via heterotrophic denitrification (Zhao et al., 2011a; Wang et al., 2009), cathodic autotrophic denitrification has some advantages over heterotrophic denitrification. Autotrophic microbial growth results in carbon dioxide fixation into biomass and little sludge production. In addition, various renewable energy technologies can be used to provide electricity to cathodic denitrification (Rabaey and Rozendal, 2010), without any need to supply EOC. To effectively combine cathodic denitrification process with renewable energy technologies, the effect of electricity current density on cathodic denitrification is central since the current densities of electricity generated from sun light and wind widely vary (EREC, 2010).

Nitrous oxide (N_2O) is an intermediate product during bacterial denitrification, N_2O emission during the biological nitrogen removal process in wastewater treatment plants (WWTPs) has been a concern due to its strong greenhouse gas effect, i.e. approximately 300 times greater per mole than that of CO_2, (Czepiel et al., 1995; Osada et al., 1995; Plósz et al., 2003; Ahn et al., 2010; Zhao et al., 2012; Gong et al., 2012a; Kampschreur et al., 2009; Foley et al., 2010). Meanwhile, our previous study suggested a new concept that N_2O recovered from WWTPs can be used as an excellent propellant resource (Scherson et al., 2013). Although many other previous studies report environmental and ecological factors affecting N_2O production from heterotrophic denitrification (Gong et al., 2012b; Betlach and Tiedje, 1981), little is known about N_2O accumulation and microbial ecology in the autotrophic BED process. In heterotrophic conditions, N_2O accumulates when EOC supply is limited while complete denitrification to N_2 occurs with sufficient EOC exposure. However, it is unclear how N_2O production is influenced by different electricity current densities in autotrophic BED in which cathodic electricity is the sole electron donor.

Cathodic denitrification has been previously studied for practical applications of BED in wastewater treatment. In addition, microbial diversity in denitrifying cathodic biofilm communities has been explored. While 454 pyrosequencing with 16S rRNA gene amplicons (at DNA level) was used to identify microbial populations of biocathode biofilms for BED system (Zhang et al., 2012), no RNA level analysis has been performed on the expression of genes of under biocathode operating conditions. In addition, there is very little information about a core microbial community for cathodic denitrification using only electrons derived from the counter electrodes. We hypothesized that a core microbial community would be selected because some members would be more efficient in electron transfer for denitrification on the cathode, and that these would be the same regardless of current densities.

Based upon the research needs discussed above, the research objectives of this work were (i) investigating the effect of electricity current density on N_2O generation during autotrophic BED process; and (ii) improving understanding of the dynamics of active microbes and their functional gene expressions in response to different current densities. Laboratory experiments were conducted using continuous-flow BED reactors to explore the effect of varying electricity current densities on the rates and N-stoichiometry of nitrate removal and N_2O production. RNA-based quantitative PCR (qPCR) and pyrosequencing were performed to determine the active microbes and denitrifying gene expressions in response to different current densities.

2. Material and methods

2.1. Experimental set-up and operation

Experiments were carried out with six identical BED reactors of a continuous-flow-mode with a hydraulic retention time (HRT) of 3.5 h (Fig. 1). Two control BED experiments were also run, i.e., one was no electricity control, and the other was no biomass control. Each BED reactor was constructed from a

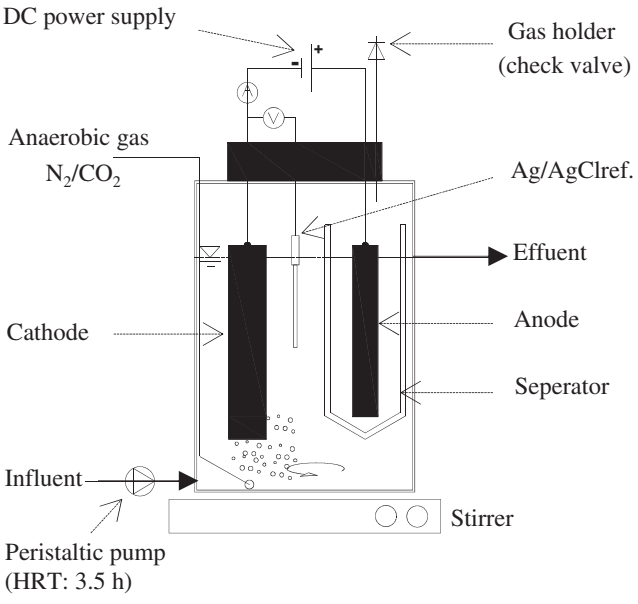

Fig. 1 – A scheme of the continuous flow BED (bioelectrochemical denitrification) reactors used in this work.

450 mL polypropylene plastic bottle, including a headspace of 90 mL to trap gases produced during operation. In a single chamber of each BED reactor, a graphite anode with a projected area of 10 cm^2 was placed together with a cathode (with a volumetric size of 25 cm^3) made of carbon felt on which BED biofilm was developed. To minimize bacterial transfer from the cathode to the anode, the anode was placed in a sponge tube (Fig. 1). A modified artificial wastewater medium (He et al., 2005) with ca. 40 mg NO_3^-–N/L (but no organic carbon source) was supplied continuously into each BED reactor. A single output DC power supply (Agilent Model U8001A) was used to poise the electrodes with the modification (Bond, 2007). Ag/AgCl reference electrodes (3.5 M KCl [Accumet®, Cat. No. 13-620-216), ca. +197 mV vs. NHE] – biological standard potential (Bard and Faulkner, 2001) were used to monitor potential of electrodes. A potentiometer (used as a rheostat with max. 100 Ω) was connected to the BED reactors in series. A digital multimeter (DMM-Agilent model 34970A) was connected to USB/GPIB interface (Agilent 82357B) was used to record potentials and currents during the experiments. A biological grade anaerobic gas (N_2:CO_2 = 80:20 (v/v), Bond (2007)) was intermittently supplied to each BED reactor, CO_2 gas of the anaerobic gas was provided as a buffering agent and as an inorganic carbon source. Temperature of reactors was at 25 ± 2 °C, and pH was maintained in a range of 6.8–7.5 during experiments.

An inoculum was taken from a recycled activated sludge of a wastewater treatment plant (Seonam, Seoul, South Korea) for seeding a BED batch reactor. This BED batch reactor was fed with acetate, hydrogen gas, 40 mg NO_3^-–N/L in the same mineral medium, and potential across electrodes poised at 0.5 V to develop cathodic biofilm. After the inoculation, each continuous flow BED reactor was received a piece (25 cm^3 with an attached wire) of biofilm developed cathode of the BED batch reactor. Then these reactors were operated with zero organic carbon environment and poised electrodes. Under the autotrophic conditions, five current densities of ca. 0.2, 1, 5, 10 and 20 mA/cm^2 were applied manually by elevating potential across the electrodes from 1 to 5 V using the single output DC power supply (Agilent Model U8001A) to poise the electrodes. Each current density was maintained for 8–9 days prior to sampling for the following nucleic acids analysis. It was confirmed that the measured effluent nitrate and nitrite concentrations were stabilized within 4 days (see Supplementary Table 1). Shifting current density was conducted in order of ca. 0.2. 1, 5, 10, 20 A/m^2. To take cathodic biofilm samples for the following molecular analysis, one reactor was sacrificed for each current density experiment.

2.2. Chemical analyses

DO (dissolved oxygen) and pH were measured using a DO meter (LabNavigator Multiparameter Meter (YO-98765-00), Colparmer USA). Oxygen in the headspace was monitored by an OxyBaby meter (Witt-Gasetechnik, Germany). To measure conductivity, a bench-top ORION was used for adjusting the flushing rate of mixed gas (Logan, 2012). Nitrate and nitrite were analyzed using Liquid Chromatography DIONEX 1100, with column AS14S and NaOH solution for eluent. For analyzing gases from the BED reactors, after a temporal stopping of influent flow for 2 h, the accumulated headspace gases were captured in gas bags (ColeParmer, USA) by flushing with helium (99.99% in purity) for 30 min. Hydrogen in the collected gas was analyzed using a portable hydrogen meter (SENKO® SP2nd, Korea). For N_2O analysis, we used a Varian-3800 gas chromatography (GC), from an Environmental Ecology Laboratory (EEL) of Yonsei university, Seoul Korea, installed with a FID and (a ^{63}Ni-electron capture detector (300 °C), and a separating column (Co. no. TM0319 from Varian, a Hayesep Q 80–100 mesh, dimension of 1 m × 1/8 inch × 2 mm). Nitrogen as a carrier gas was flowing at 60 mL/min at 30 psi and the oven was maintained at 50 min/20 min/cycle. The electron flow supplied to cathode was calculated by using the equation: Charge (Coulombs) = Current (A) × Time (s). The charges (C) value was converted to the number of electron mole by dividing Faraday constant: electron (mole of e^-) = Charge (C)/F (96,485 C/mole of e). For Kinetics analysis of nitrate removal rates and N_2O accumulations, we applied Michaelis–Menten model fittings using non-linear regression (SigmaPlot 12.0), with the regression equation: $R = V_{max}{}^{*}A/(K_m + A)$, with R stands for removal or accumulation rate, V_{max} for Maximum of removal/accumulation, A for current density and K_m for half saturation rate.

2.3. RNA extraction and cDNA synthesis

For each current density experiment, cathode biofilm was collected as described above, rinsed with a neutral buffer solution, dissected into 2 cm × 10 cm pieces and then placed immediately into RNA*later*® and stored at −20 °C prior to the following RNA extraction. To completely detach cells from the electrodes, the biofilm stored in RNA*later*® was three times sonificated for 3 s (Sonic & Materials, CT, USA). The cell suspension was centrifuged immediately at 13,000× *g* for 3 min at 4 °C. Total RNA was extracted using the RNA PowerSoil total RNA isolation kit (MO BIO Laboratories, CA, USA). Following the extraction, RNA was further purified by using the Turbo DNA-free kit (Ambion, CA, USA) and the Rneasy Minelute Cleanup kit (Qiagen, CA, USA) to remove co-extracted DNA and other protein contamination. cDNA synthesis from the purified RNA was performed using the Superscript III First-Strand Synthesis SuperMix (Invitrogen, CA, USA).

2.4. Pyrosequencing analysis

Universal primers encompassing the V1–V3 region, 27F (GAGTTTGATCMTGGCTCAG), and modified 518R (WTTAC CGCGGCTGCTGG), were used for amplifying the 16S rRNA genes (Muyzer et al., 1993). Each PCR reaction was carried out with three of the 25 μL reaction mixtures containing 100 ng of cDNA, 10 μM of each primer (BIONEER, Seoul, Korea), and AccuPrimeTM Taq DNA Polymerase High Fidelity (Invitrogen, WI, USA) to obtain the following final concentrations: 1.25 U of Taq polymerase, 50 mM of $MgSO_4$, and 10× of the PCR buffer. A C1000TM thermal cycler (BIO-RAD, CA, USA) was used for PCR as follows: (i) an initial denaturation step at 94 °C for 3 min, (ii) 25 cycles of annealing and extending (each cycle occurred at 94 °C for 1 min followed by 54 °C for 30 s and an extension step at 68 °C for 1 min), and (iii) the final extension at 68 °C for 5 min. After PCR amplification, the amplicons were purified

once by gel electrophoresis and twice using QIAquick Gel extraction (Qiagen, CA, USA) and QIAquick PCR purification kits (Qiagen, CA, USA). In order to recover a sufficient amount of purified amplicon, three 25-μl reaction mixtures were combined into one mixture prior to amplicon purification. Purified amplicons were pyrosequenced by Macrogen Inc, Seoul.

Sequences were analyzed following the modified protocol suggested by Schloss et al. (2011) using Mothur (Schloss et al., 2009). Using multiplex identifier sequences, we sorted the flowgram files (.flow) with more than 1 mismatch to the barcode, 2 mismatches to the primer, an ambiguous nucleotide, flows between 450 and 720 flows. Flowgrams were corrected and translated to DNA sequences using shhh.flows command as the implemented version of Pyronoise in Mothur (Quince et al., 2009). Chimera sequences were removed by applying the Uchime algorithm with self-references (Edgar et al., 2011). To remove or/and reduce PCR amplification and sequencing errors, sequences were denoised using shhh.seqs in Ampiconnoise (Quince et al., 2011).

We merged sequences from processed sequences and made a group file to recognize the samples. Unique sequences were aligned to Silva Gold aligned sequences and trimmed to include comparable regions. To generate operational taxonomic units (OTUs) at 0.03 distances, we produced a distance matrix and clustered them using the farthest algorithm. Sequences were classified using the Ribosomal Database Project training set version 7 with a threshold of 50%. Classified sequences were analyzed into phylotype at class and genus level. We estimated OTU Richness, Shannon index and Evenness (Magurran, 2004; Jost, 2006). We used one-way ANOVA to determine the significant difference of microbial diversity between biofilm with different current densities and inoculum. A taxonomy-supervised dendrogram was constructed to compare microbial communities from samples using relative abundances (Sul et al., 2011). After calculating relative abundances of genera, including unclassified sequences, we produced a distance matrix (vegdist) and clustered them through the average algorithm (hclust) using Vegan package from R.

To test for statistical associations between five different current densities and the abundance of the core genera, we ranked the abundance of the core genera in their current densities. Each abundance was assigned a ranking from 1 (largest abundance) to 5 (smallest abundance) for each current density. We then used Spearman's rank correlation to test for statistical associations among the rankings of the individual abundance of the core genera and current density (Helbling et al., 2012).

2.5. *Real-time PCR analysis*

The real-time PCR assay was performed on a BIORAD iQ5 (BIORAD, CA, USA). Amplification reactions were performed in a volume of 25 μL and the reaction mixture contained 12.5 μL iQ™ SYBR Green Supermix (BIORAD, CA, USA), 1 μL of each primer (10 mM), 10 ng of total cDNA, and RNase-free water. The primer sets for amplification of 16S rRNA and denitrifying functional genes is summarized in Table 1. The thermocycling steps for qPCR for 16S rRNA amplification included 95 °C for 30 s, 40 cycles at 95 °C for 15 s, 53 °C for 20 s, and 72 °C for 20 s. The qPCR conditions for the *narG* and *napA* amplification were 15 min at 95 °C; six cycles consisting of 30 s at 95 °C and 30 s at 63 °C, with a touchdown of −1 °C bin each cycle; and 40 cycles consisting of 30 s at 95 °C, 30 s at 58 °C (61 °C for *napA*), 30 s at 72 °C, and 30 s at 80 °C (Bru et al., 2007). The *nirS*, *nirK* and *norB* qPCR amplification conditions included 50 °C for 2 min, 95 °C for 10 min, and 40 cycles at 95 °C for 1 min, 50 °C for 1 min, and 60 °C for 1 min (Geets et al., 2007). Lastly, qPCR amplification of *nosZ* included an initial cycle of 95 °C for 15 min; six cycles of 95 °C for 15 s, 67 °C for 30 s with a touchdown of −1 °C in each cycle, 72 °C for 30 s, and 80 °C for 15 s; 40 cycles of 95 °C for 15 s and 62 °C for 15 s, 72 °C for 30 s, and 80 °C for 15 s; and 1 cycle at 95 °C for 15 s and 60 °C for 15 s, to 95 °C for 15 s (Henry et al., 2006). In all experiments, three replicate amplifications were performed and with appropriate negative controls containing no template DNA.

3. Results

3.1. *Nitrogen reduction and nitrous oxide accumulation at different current densities*

At the same loading rate of around ca. 1.7 g/NCCm^3.h, nitrate removal rate increased with increased current density until reaching plateau at ~10 A/m^2 (Fig. 2). Nitrite accumulated at the current density of 5 A/m^2, but was removed at 10 A/m^2.

Table 1 – Primer sets for denitrifying pathway genes used in this study.

Gene	Primer name	Sequence (5′ → 3′)	Reference
napA	V17m	TGGACVATGGGYTTYAAYC	Bru et al. (2007)
	napA4r	ACYTCRCGHGCVGTRCCRCA	
narG	narG-f	TCGCCSATYCCGGCSATGTC	Bru et al. (2007)
	narG-r	GAGTTGTACCAGTCRGCSGAYTCSG	
nirS	nirS cdAF	GTSAACGTSAAGGARACSGG	Geets et al. (2007)
	nirS R3cd	GASTTCGGRTGSGTCTTGA	
nirK	nirK 1F	GGMATGGTKCCSTGGCA	Geets et al. (2007)
	nirK 5R	GCCTCGATCAGRTTRTGGTT	
norB	cnorB-2F	GACAAGNNNTACTGGTGGT	Geets et al. (2007)
	cnorB-6R	GAANCCCCANACNCCNGC	
nosZ	nosZ 2F	CGCRACGGCAASAAGGTSMSSGT	Henry et al. (2006)
	nosZ 2R	CAKRTGCAKSGCRTGGCAGAA	

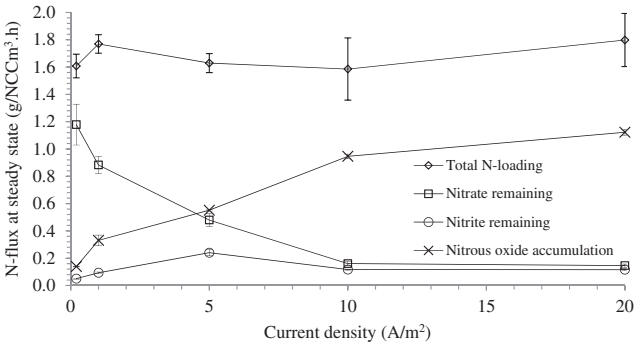

Fig. 2 – Nitrate, nitrite, and N_2O fluxes at different cathodic current densities.

The total nitrogen removal rate was 0.43, 0.89, 1.15, 1.43 and 1.65 NO_3^--N (g/NCCm^3.h) at 0.2, 1.0, 5.0, 10.0 and 20.0 A/m^2, respectively (Fig. 3), showing a saturation trend of nitrate removal rates in response to increasing current densities. Meanwhile, increasing current density had similar effects on the accumulation of N_2O (Fig. 3). The conversion ratios of the accumulated N_2O from the reduced nitrate also increased with increase in current density, ranging from 30% (at 0.2 A/m^2) to 70% (at 20 A/m^2).

To further examine the effect of current densities on the rates of nitrate removal and N_2O accumulation, non-linear regression analysis was performed with Michaelis–Menten type kinetic model. The model fits well with the observations (Suppl. Fig. 1), with relatively high R^2 values (0.9733 and 0.9458 for nitrate removal rates and N_2O accumulation rates, respectively), indicating that the current density dependent rates of nitrate removal and N_2O accumulation follow saturation kinetics (Table 2). The *p*-values for maximal rate (i.e., V_{max}) estimation were lower than those for the half saturation constant (K_m) estimation, indicating higher certainty in the maximal rate estimation. The maximum removal rate for nitrate (V_{max} of 1.46 g/m^{3}h) and the maximum accumulation rate for N_2O (V_{max} of 1.43 g/m^{3}h) are almost identical while K_m values for nitrate removal (0.67 A/m^2) and N_2O accumulation (5.71 A/m^2) were inconsistent. These kinetic parameter results

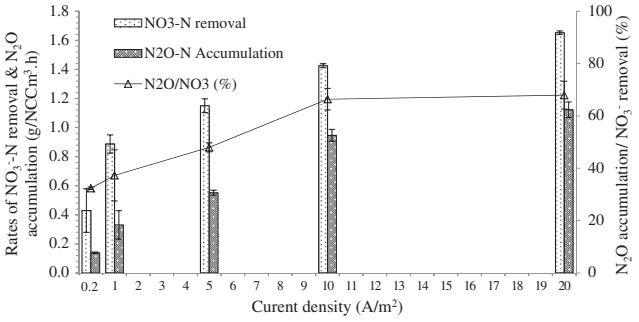

Fig. 3 – The effects of different current densities on the rates of NO_3^- removal and N_2O accumulation (left Y-axis) and the ratios of N_2O–N accumulated among N-nitrate removed (solid line – right Y-axis).

confirm the observations that the conversion ratios of the accumulated N_2O from the reduced nitrate increased with increase in current density.

3.2. *Active microbial community diversity and population dynamics*

3.2.1. *Microbial diversity of active BED microbes*

Microbial diversities in active BED microbes were analyzed using amplification then pyrosequencing of expressed 16S rRNA genes. As indicated by the results of OTU Richness, Shannon index and evenness (Table 3), the low current densities (0.2 and 1.0 A/m^2) resulted in reduced alpha-diversity, being lower than the inoculum (*p*-values <0.001) while the higher current densities (5.0. 10.0 and 20.0 A/m^2) resulted in relatively high diversities, which are comparable to that of the inoculum.

The beta-diversity of the active microbial communities at different current densities was assessed using the Bray–Curtis index of similarity (Fig. 4). Expressed RNA-based 16S rRNA dendrogram revealed that active community composition clustered into three separate groups (0.2 and 1.0 A/m^2 [low], 5.0 and 10.0 A/m^2 [medium] and 20.0 A/m^2 [high]), depending on the different current density levels. Similarly, the composition of expressed *nirK* genes also separately clustered according to different current densities. Although no *nirK* data were available for the inoculum, the trees without the inoculum showed a consistent trend between 16S rRNA and *nirK* data. These confirm the conclusion from the expressed 16S rRNA dendrogram.

3.2.2. *Finding of an core active BED community*

A core active BED community was observed under the autotrophic conditions. If the relative abundance of a genus member was higher than 0.1%, the genus member was considered as 'detected'. The core community contains the genus members that were active at all the applied current densities ("5 Shared" in Fig. 5), accounting 5.4% of the total 298 genera. The relative abundances of the core members were decreased with increase in current density, ranging from 58.2% to 28.8%. The overall relative abundance of the core active members tends to decrease with increase in current density.

Sixteen genera were identified as core members (Table 4). Compared to the inoculum from the heterotrophic BED reactor, thirteen members out of the sixteen core members showed increased detections during the autotrophic BED reactor operations, with a few exceptions of *Longilinea*, Unclassified *Comamonadaceae* and Unclassified *Solirubrobacterales*.

To identify bacteria members that exhibited activities positively correlating with increase in current density, Spearman's rank correlation test was performed with that genus members that were detected in common at least three different current densities (Table 5). The identified genera were *Alicycliphilus*, *Gemmatimonas*, *Acidovorax*, *Simplicispira*, *Thermomonas*, *Aeromona*, *Flavobacterium*, and *Stenotrophomonas*. All of them are gram negative bacteria. In addition, *Acidovorax*, *Aeromonas*, *Alicycliphilus*, *Flavobacterium*, *Simplicispira*, *Stenotrophomonas* and *Thermomonas* are iron-reducing or oxidizing bacteria as well as nitrate or nitrite reducers (Wrighton et al.,

Table 2 – Results of Michaelis-Menten-type model fittings using non-linear regressions.

	Nitrate removal			Nitrous oxide accumulation		
Coefficient	Average	STDEV	*p*-value	Average	STDEV	*p*-value
V_{max} (g/m^{3}h)	1.46	0.07	0.0002	1.43	0.26	0.0123
K_m (A/m^2)	0.67	0.16	0.0239	5.71	2.92	0.1457
R^2	0.9733			0.9458		

2010; Weelink et al., 2008; Straub et al., 2004; Ivanov et al., 2005; Cao et al., 2012).

3.2.3. *Effect of current density on the expression of the denitrifying pathway genes*

Electricity current density also affected the expressions of denitrifying pathway genes. The ratios of the mRNA (cDNA) copies of the denitrifying genes *napA*, *narG*, *nirS*, *nirK*, *norB* and *nosZ* to the copies of total 16S rRNA genes (at DNA level) were estimated for the different current densities (Fig. 6). The gene expressions of *napA* and *nirS* were comparable to the levels for the inoculum exhibiting a sufficient denitrification up to nitrogen gas. In the cases of *narG* and *nirK*, their gene expressions were weaker than the inoculum at the low current densities (0.2 or/and 1.0 A/m^2) while the gene expressions for the medium and high current densities (above 5.0 A/m^2) reached plateau levels, which are similar to those for the inoculum. In the case of *norB*, peak values of gene expressions were observed in the medium current densities (5.0 and 10.0 A/m^2). The peak values were similar to that for the inoculum but the gene expressions for the low and high current densities were lower than that for the inoculum. Unlike other denitrification genes, *nosZ* genes were under-expressed compared to that of the inoculum, regardless of the current density values.

4. Discussion

4.1. *Nitrogen removal and comparison with other systems*

The highest denitrification rate was 1.65 NO_3^-–N (g/NCCm^3.h) at ca. 20.0 A/m^2 current density (Table 3) which is three times higher than the 0.44 NO_3^-–N (g/NCCm^3.h) obtained by Feng et al. (2013). We even bettered the results they obtained of 0.95, 1.0, 1.1 NO_3^-–N (g/NCCm^3.h) using methanol, glucose, and starch as organic carbon sources. Our removal rate is also greater than the rate obtained by Gregory et al. (2004) in BED, 0.83 NO_3^-–N (g/TCCm^3.h). Park et al. (2005) obtained a maximal denitrification rate in the order of 0.75 NO_3^-–N (g/TCCm^3.h) in their biological cathodic denitrification system with an abiotic anode driven by a power supply. Virdis et al. (2010) achieved maximum 4.8 NO_3^-–N (g/TCVm^3.h) removal using organic carbon sources. But as mentioned previously, the use of organic carbon sources creates problems of fast growth causing clogging and difficulties in sludge disposal and toxic residuals (Ghafari et al., 2008). We used CO_2/$NaHCO_3$ to favor autotrophic denitrification which has the advantage of low microbial biomass and organic products, so limited secondary pollution, i.e. dissolved organic carbons (Zhao et al., 2011b). The improved results obtained from this study could come from better pH buffering capacity to neutralize the alkalinity caused by denitrification. This pH increase noted by Popat et al. (2012) mostly accounts for losses in effectiveness of BES.

Recent studies on effects of carbon source on BED performance show that adding organic carbon sources could improve nitrate removal rates. Cooperative heterotrophic and autotrophic denitrification has shown higher removal efficiency (Suppl. Table 2). Compared with autotrophic denitrification, the obvious superiority lies in a larger treatment capacity and high removal efficiency. Lower organic carbon source utilization and the absence of organic pollution make the process better than full heterotrophic denitrification. Our system is also superior to other previous systems in terms of less biosolids, more uptake (sequestration) of CO_2 and a comparatively high removal efficiency. Therefore, application

Table 3 – Alpha-diversities in response to different current densities.

Sample	No. sequences (filtered)	OTU richness	Shannon index	Evenness
Inoculum	3110	603 ± 16	6.51 ± 0.10	0.91 ± 0.02
0.2 A/m^2	1640	372 ± 8	5.24 ± 0.06	0.81 ± 0.01
1.0 A/m^2	2779	543 ± 10	6.05 ± 0.04	0.84 ± 0.01
5.0 A/m^2	1075	636 ± 24	6.75 ± 0.12	0.94 ± 0.02
10.0 A/m^2	984	607 ± 13	6.52 ± 0.09	0.91 ± 0.01
20.0 A/m^2	998	634 ± 17	6.62 ± 0.11	0.89 ± 0.01

Note: OTU Richness was estimated from a sub-sample of 984 sequences randomly selected from the filtered sequences.

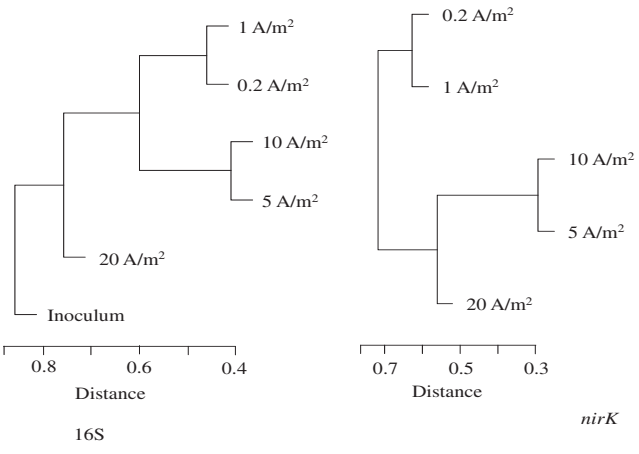

Fig. 4 – Beta-diversities for the expressed 16S rRNA and *nirK* in response to different current densities.

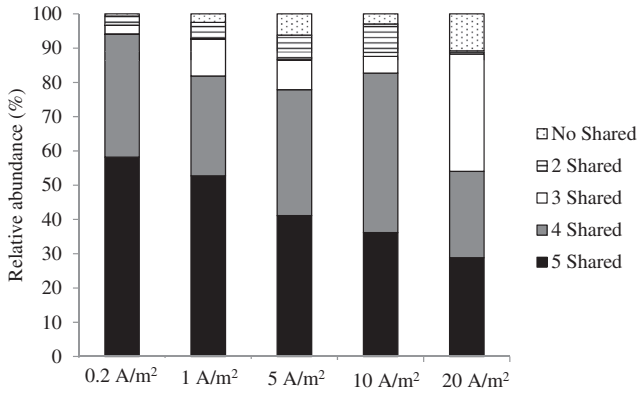

Fig. 5 – Relative abundances of core bacterial genus members ("5 Shared") from the active BED communities in response to different current densities. The "5 Shared" indicates that the corresponding genus members were commonly detected at the 5 current densities applied in this work. The "No Shared" genus members were detected only at a single current density while the "4 Shared", "3 Shared" and "2 Shared" genus members were detected at multiple current densities among the applied densities.

of our BED could help lessen cost and be applicable for low nitrate strength source wastes and a strict requirement of no waste generation.

4.2. *Nitrous oxide accumulation in response to current density*

N_2O accumulation during biological denitrification has been widely explored. However, this is the first report N_2O accumulation by BED under autotrophic conditions. N_2O accumulation is of special interest not just because the compound is much worse global warming gas but also N_2O can be used as an excellent propellant (Scherson et al., 2013). To understand the factors affecting N_2O emission, operational parameters have been investigated, including the nitrite, and DO concentrations, sludge retention time (SRT), pH, and carbon/nitrogen (C/N) ratio (Ahn et al., 2010; Beline et al., 2001; Hanaki et al., 1992; Itokawa et al., 2001; Hwang et al., 2006; Alinsafi et al., 2008). While the previous studies provided information on environmental factor(s) influencing N_2O, this study provides information on transcriptional regulation of denitrification pathway genes under autotrophic conditions. According to the results of denitrification pathway gene expressions, *nosZ* expression level was significantly lower than that of active BED inoculum while the other denitrification genes were expressed comparable to the active denitrifying inoculum community (Fig. 6). This low expression of *nosZ* gene is a molecular explanation for N_2O accumulation.

At the high levels of current densities approximately 70 percent of the removed nitrate was transformed and accumulated into N_2O. The high percent N_2O accumulation is relatively high compared to the previous reports regarding N_2O accumulation (Scherson et al., 2013). Because of low aqueous phase solubility of N_2O, it would be easily captured in head-space and selectively concentrated (purified) via well-established size selection and/or adsorptive column separation processes (Vorotyntsev et al., 2009). Since purified N_2O can be applied for the current existing engines, the recovered N_2O from wastewater would be easily commercialized in the current market. N_2O accumulation by autotrophic BED would be a promising microbial process for the future nitrogen capture, storage and utilization (NCSU) using wastewater.

4.3. *Denitrification kinetics and gene expression characteristics*

Kinetics reveals that affinity (half saturation of current density) for nitrate and NO are different while their maximum rate constant V_{max} values are similar. This saturation kinetic behavior may be explained by denitrification pathway gene expression patterns. Since *napA* as a periplasmic nitrate reductase with a short distance to the outer membrane to connect to external electron flow compared with *narG*, which is a membrane bounded nitrate reductase, we expected increased expression of *napA* with high current densities

Table 4 – The core genus members and their relative abundances (% of total) at different current densities.

Genus member	Inoculum	0.2 A/m²	1.0 A/m²	5.0 A/m²	10.0 A/m²	20.0 A/m²
Unclassified *Rhodocyclaceae*	1.8	23.5	5.7	5.1	7.8	0.9
Unclassified *Bacteria*	5.3	21.3	35.9	6.4	6.7	2.7
Bacillus	0.0	5.1	0.6	2.7	2.0	5.4
Unclassified *Betaproteobacteria*	1.5	3.2	1.9	3.0	6.6	0.9
Nitrosomonas	0.0	1.2	0.1	0.7	1.5	0.9
Unclassified *Bacillales*	0.0	1.0	0.1	1.1	0.4	0.9
Longilinea	7.9	1.0	1.6	0.7	0.6	2.7
Unclassified *Comamonadaceae*	5.1	0.5	2.7	2.2	1.3	1.8
Gemmatimonas	0.1	0.4	0.2	1.8	2.6	1.8
Unclassified *Rhizobiales*	0.4	0.3	0.7	1.4	0.5	0.9
Unclassified *Clostridiales*	0.2	0.2	0.4	0.3	0.4	1.8
Alicycliphilus	0.0	0.1	0.1	0.6	0.2	3.6
Nitrospira	0.3	0.1	0.2	1.1	1.4	0.9
Thauera	0.0	0.1	0.7	12.7	2.9	0.9
Unclassified *Flavobacteriales*	0.3	0.1	0.3	0.2	0.3	0.9
Unclassified *Solirubrobacterales*	7.0	0.1	1.7	1.1	0.7	1.8

Table 5 – Bacterial genera exhibiting positive association with current density.

Genus	Shared	Relative abundance (%)					Coefficient	P-value
		0.2 A/m^2	1.0 A/m^2	2.0 A/m^2	5.0 A/m^2	10.0 A/m^2		
Alicycliphilus	5	0.1	0.1	0.6	0.2	3.6	0.9	0.01
Gemmatimonas	5	0.4	0.2	1.8	2.6	1.8	0.8	0.03
Acidovorax	4	0.0	0.0	0.4	0.2	0.9	0.9	0.01
Simplicispira	4	0.0	0.4	0.6	0.4	2.7	0.9	0.01
Thermomonas	4	0.0	0.3	2.9	2.1	18.0	0.9	0.01
Aeromonas	3	0.0	0.0	0.4	0.1	1.8	0.87	0.01
Flavobacterium	3	0.0	0.0	0.3	0.1	27.9	0.87	0.01
Stenotrophomonas	3	0.0	0.0	0.1	0.6	0.9	0.98	0.01

(Simpson et al., 2010). However, *napA* expression decreased with increasing current densities, whereas *narG* increased. This result may be due to gene regulation not having evolved for sensing the cathodic reductant source, or that *narG* increased consumption of their favorable electron donors, not for respiration, but for cellular ATP and biochemical production (Pandit and Mahadevan, 2011). The gene expression data for the nitrate reductase genes may explain for the observed nitrate removal kinetics as a function of electricity current densities.

The rate limiting step in the whole denitrification pathway was found to be NO reductase (*nosZ*). Denitrification intermediates other than N_2O were not accumulated. After the reduction of nitrate into nitrite, nitrite was not accumulated at the all current densities. This is also confirmed by the following nitrite reductase gene expression data, i.e., the gene expression of *nirK* and *nirS* gradually increased with current densities increased and gotten saturation exhibiting a fully expressed level observed in the inoculum control. The byproduct from the nitrite reductase activity, NO might have not been accumulated due to the compound is unstable and easily transformed into N_2O or other forms via abiotic process. In addition, the *norB* expression data suggest that biological transformation of NO into N_2O might have been significantly activated. Finally, N_2O accumulation and the low expression of *nosZ* gene support the conclusion that NO-to-N_2O transformation was the rate limiting step in the whole denitrification pathway.

4.4. *A core community in different electricity current densities*

As shown by the pyrosequencing of amplicons from expressed 16S rRNA and *nirK*, the structures of active BED biofilm communities were influenced with different current densities. This suggests that current density is an operational

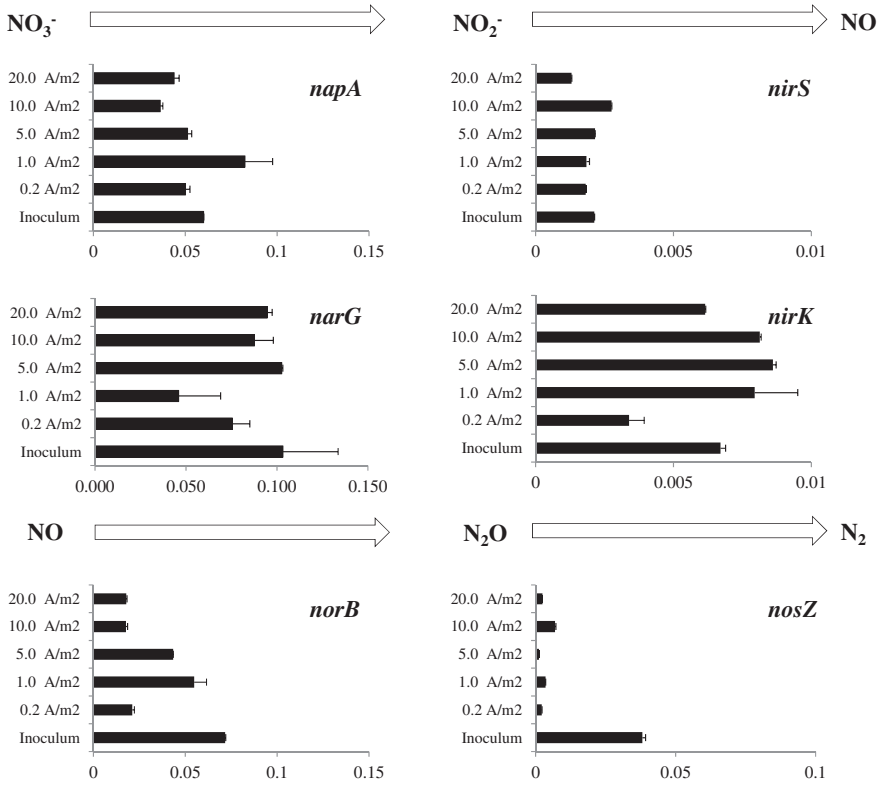

Fig. 6 – Ratios of denitrifying pathway gene copies (cDNA from mRNA) to 16S rRNA gene copies (DNA), and X-axis is in dimensionless.

factor influencing the beta-diversity of active BED communities under autotrophic conditions.

Although the microbial composition of the biofilm changed with changes in current densities, we hypothesized the certain member of the active microbial community would be selected by these conditions and hence be more efficient in electron transfer and denitrification on the cathode, regardless of current densities. In this study, we could identify such core bacterial genus members as taxa shared at all current densities (Table 4). In addition, most of them were more activated than the inoculum. The findings suggest that the identified core members may be bioelectrochemically active denitrifiers under autotrophic conditions. This implicates that stimulating the core community members would be beneficial for improving the stability of nitrate removal and N_2O production in autotrophic BED processes, especially when electricity generation is unstable, which is typical in the present renewable energy technologies such as wind, solar, microbial fuel cells etc.

The Spearman's rank correlation test with the bacterial genus members detected in multiple current densities could identify the eight active bacterial members that exhibited positive association with increase in current density (Table 5). All of them are gram negative bacteria. Jung and Regan (2007) suggested gram negative bacteria would have a higher capacity in electron transfer, compared to gram positive bacteria. Furthermore, a recent study showed that iron-reducing or oxidizing bacteria are electrochemically active and play an important role in electron transfer to electrodes (Kim et al., 2005). *Acidovorax*, *Aeromonas*, *Alicycliphilus*, *Flavobacterium*, *Simplicispira*, *Stenotrophomonas* and *Thermomonas* are iron-reducing or oxidizing bacteria as well as nitrate or nitrite reducers (Wrighton et al., 2010; Weelink et al., 2008; Straub et al., 2004; Ivanov et al., 2005; Cao et al., 2012). These results support the concept that these bacteria coexist for high capacity electron transfer on the cathode to drive denitrification.

To evaluate the trends in nitrate and nitrite reduction, further characterization of other electron donors such as biochemical productions by microbial electro-synthesis is needed. Although the BED reactors in this study were not operated at optimal cathode potential, i.e. a potential near zero as suggested by Clauwaert et al. (2007) for complete denitrification, denitrifying genes related with reductive steps of denitrification process (NO_3^- to NO_2^-) were significantly associated with current densities (except for *nirK*), whereas current densities showed no association with subsequent denitrification steps (NO_3^- to N_2). It is clear that current dose has an important effect on nitrate and nitrite reduction under autotrophic conditions.

5. Conclusions

- This is the first to report the accumulation of N_2O from bioelectrochemical denitrification in a zero organic carbon wastewater condition. As the current density increased, the accumulation of N_2O increased up to approximately 70% of the removed nitrate. In addition, the rates of nitrate removal and N_2O accumulation in response to varying current densities follow Michaelis-Menten-type kinetics.
- According to the 16S rRNA gene-targeted pyrosequencing results, the structures of active BED biofilm communities were significantly influenced with different current densities. Nevertheless, a core bacterial community was found to co-exist in the bioelectrochemically active biofilms regardless of different current densities. Most of the core active members may have been bioelectrochemically active denitrifiers under autotrophic conditions.
- The effects of different current densities on the gene expressions of denitrificaiton pathway were also characterized in the bioelectrochemically active cathode biofilms under autotrophic conditions. The gene expression for nitric oxide reduction (*norB*) was dynamically regulated depending upon the different current densities. Meanwhile, at all the current densities, the genes for nitrate reduction and nitrite reduction were expressed (*nap*A, *nar*G, *nir*S and *nir*K) while the gene for N_2O reduction (*nos*Z) was repressed. The repressive effect of cathodic electron current on the *nos*Z gene expression is a molecular explanation for the accumulation of N_2O in the bioelectrochemical denitrification process in zero organic carbon environment.
- The findings of the kinetic and gene expression investigation are useful in further optimizing bioelectrochemical denitrification processes for removing nitrate and recovering N_2O as a combustion propellant from no BOD-containing wastewater. In addition, stimulating the core community members would be beneficial for improving the stability of nitrate removal and N_2O production in autotrophic BED processes when electricity supply fluctuates.

Acknowledgments

This research was supported by the WCU (World Class University) Program of the National Research Foundation of Korea, funded by the Ministry of Education, Science and Technology (R33-10076).

Appendix A. Supplementary data

Supplementary data related to this article can be found at http://dx.doi.org/10.1016/j.watres.2013.08.041.

REFERENCES

Ahn, J.H., Kim, S., Park, H., Rahm, B., Pagilla, K., Chandran, K., 2010. N_2O emissions from activated sludge processes, 2008–2009: results of a national monitoring survey in the united states. Environ. Sci. Technol. 44 (12), 4505–4511.

Alinsafi, A., Adouani, N., Béline, F., Lendormi, T., Limousy, L., Sire, O., 2008. Nitrite effect on nitrous oxide emission from denitrifying activated sludge. Process Biochem. 43 (6), 683–689.

Bard, A.J., Faulkner, L.R., 2001. Electrochemical Methods: Fundamentals and Applications.

Beline, F., Martinez, J., Marol, C., Guiraud, G., 2001. Application of the ^{15}N technique to determine the contributions of

nitrification and denitrification to the flux of nitrous oxide from aerated pig slurry. Water Res. 35 (11), 2774–2778.
Betlach, M.R., Tiedje, J.M., 1981. Kinetic explanation for accumulation of nitrite, nitric oxide, and nitrous oxide during bacterial denitrification. Appl. Environ. Microbiol. 42 (6), 1074–1084.
Bond, D.R., 2007. In: Hurst, C.J., Crawford, R.L., Garland, J.L., Lipson, D.A., Mills, A.L., Stetzenbach, L.D. (Eds.), Manual of Environmental Microbiology, pp. 1143–1144.
Bru, D., Sarr, A., Philippot, L., 2007. Relative abundances of proteobacterial membrane-bound and periplasmic nitrate reductases in selected environments. Appl. Environ. Microbiol. 73 (18), 5971–5974.
Cao, F., Liu, T.X., Wu, C.Y., Li, F.B., Li, X.M., Yu, H.Y., Tong, H., Chen, M.J., 2012. Enhanced biotransformation of DDTs by an iron- and humic-reducing bacteria Aeromonas hydrophila HS01 upon addition of goethite and anthraquinone-2,6-disulphonic disodium salt (AQDS). J. Agric. Food Chem. 60 (45), 11238–11244.
Cheng, K.Y., Ginige, M.P., Kaksonen, A.H., 2012. Ano-cathodophilic biofilm catalyzes both anodic carbon oxidation and cathodic denitrification. Environ. Sci. Technol. 46 (18), 10372–10378.
Clauwaert, P., Rabaey, K., Aelterman, P., de Schamphelaire, L., Pham, T.H., Boeckx, P., Boon, N., Verstraete, W., 2007. Biological denitrification in microbial fuel cells. Environ. Sci. Technol. 41 (9), 3354–3360.
Czepiel, P., Crill, P., Harriss, R., 1995. Nitrous oxide emissions from municipal wastewater treatment. Environ. Sci. Technol., 2352–2356.
Edgar, R.C., Haas, B.J., Clemente, J.C., Quince, C., Knight, R., 2011. UCHIME improves sensitivity and speed of chimera detection. Bioinformatics 27 (16), 2194–2200.
EREC, 2010. Renewable Energy in Europe: Markets, Trends and Technologies.
Feng, H., Huang, B., Zou, Y., Li, N., Wang, M., Yin, J., Cong, Y., Shen, D., 2013. The effect of carbon sources on nitrogen removal performance in bioelectrochemical systems. Bioresour. Technol. 128 (0), 565–570.
Foley, J., de Haas, D., Yuan, Z., Lant, P., 2010. Nitrous oxide generation in full-scale biological nutrient removal wastewater treatment plants. Water Res. 44 (3), 831–844.
Geets, J., de Cooman, M., Wittebolle, L., Heylen, K., Vanparys, B., De Vos, P., Verstraete, W., Boon, N., 2007. Real-time PCR assay for the simultaneous quantification of nitrifying and denitrifying bacteria in activated sludge. Appl. Microbiol. Biotechnol. 75 (1), 211–221.
Ghafari, S., Hasan, M., Aroua, M.K., 2008. Bio-electrochemical removal of nitrate from water and wastewater – a review. Bioresour. Technol. 99 (10), 3965–3974.
Gong, Y.-K., Peng, Y.-Z., Yang, Q., Wu, W.-M., Wang, S.-Y., 2012a. Formation of nitrous oxide in a gradient of oxygenation and nitrogen loading rate during denitrification of nitrite and nitrate. J. Hazard. Mater. 227–228 (0), 453–460.
Gong, Y.K., Peng, Y.Z., Yang, Q., Wu, W.M., Wang, S.Y., 2012b. Formation of nitrous oxide in a gradient of oxygenation and nitrogen loading rate during denitrification of nitrite and nitrate. J. Hazard Mater. 227–228, 453–460.
Gregory, K.B., Bond, D.R., Lovley, D.R., 2004. Graphite electrodes as electron donors for anaerobic respiration. Environ. Microbiol. 6 (6), 596–604.
Hanaki, K., Hong, Z., Matsuo, T., 1992. Production of nitrous oxide gas during denitrification of wastewater. Water Sci. Technol. 26 (5–6), 1027–1036.
He, Z., Minteer, S.D., Angenent, L.T., 2005. Electricity generation from artificial wastewater using an upflow microbial fuel cell. Environ. Sci. Technol. 39 (14), 5262–5267.
Helbling, D.E., Johnson, D.R., Honti, M., Fenner, K., 2012. Micropollutant biotransformation kinetics associate with WWTP process parameters and microbial community characteristics. Environ. Sci. Technol. 46 (19), 10579–10588.
Henry, S., Bru, D., Stres, B., Hallet, S., Philippot, L., 2006. Quantitative detection of the nosZ gene, encoding nitrous oxide reductase, and comparison of the abundances of 16S rRNA, narG, nirK, and nosZ genes in soils. Appl. Environ. Microbiol. 72 (8), 5181–5189.
Hwang, S., Jang, K., Jang, H., Song, J., Bae, W., 2006. Factors affecting nitrous oxide production: a comparison of biological nitrogen removal processes with partial and complete nitrification. Biodegradation 17 (1), 19–29.
Itokawa, H., Hanaki, K., Matsuo, T., 2001. Nitrous oxide production in high-loading biological nitrogen removal process under low cod/n ratio condition. Water Res. 35 (3), 657–664.
Ivanov, V., Stabnikov, V., Zhuang, W.Q., Tay, J.H., Tay, S.T., 2005. Phosphate removal from the returned liquor of municipal wastewater treatment plant using iron-reducing bacteria. J. Appl. Microbiol. 98 (5), 1152–1161.
Jost, L., 2006. Entropy and diversity. Oikos 113 (2), 363–375.
Kampschreur, M.J., Temmink, H., Kleerebezem, R., Jetten, M.S.M., van Loosdrecht, M.C.M., 2009. Nitrous oxide emission during wastewater treatment. Water Res. 43 (17), 4093–4103.
Kim, J.R., Min, B., Logan, B.E., 2005. Evaluation of procedures to acclimate a microbial fuel cell for electricity production. Appl. Microbiol. Biotechnol. 68 (1), 23–30.
Logan, B.E., 2012. Essential data and techniques for conducting microbial fuel cell and other types of bioelectrochemical system experiments. Chemsuschem 5 (6), 988–994.
Logan, B.E., Hamelers, B., Rozendal, R., Schroder, U., Keller, J., Freguia, S., Aelterman, P., Verstraete, W., Rabaey, K., 2006. Microbial fuel cells: methodology and technology. Environ. Sci. Technol. 40 (17), 5181–5192.
Magurran, A.E., 2004. Measuring biological diversity. Afr. J. Aquat. Sci. 29 (2), 285–286.
Muyzer, G., de Waal, E.C., Uitterlinden, A.G., 1993. Profiling of complex microbial populations by denaturing gradient gel electrophoresis analysis of polymerase chain reaction-amplified genes coding for 16S rRNA. Appl. Environ. Microbiol. 59 (3), 695–700.
Osada, T., Kuroda, K., Yonaga, M., 1995. Reducing nitrous oxide gas emissions from fill-and-draw type activated sludge process. Water Res. 29 (6), 1607–1608.
Pandit, A.V., Mahadevan, R., 2011. In silico characterization of microbial electrosynthesis for metabolic engineering of biochemicals. Microb. Cell Fact 10, 76.
Pant, D., Singh, A., Van Bogaert, G., Irving Olsen, S., Singh Nigam, P., Diels, L., Vanbroekhoven, K., 2012. Bioelectrochemical systems (BES) for sustainable energy production and product recovery from organic wastes and industrial wastewaters. RSC Adv. 2 (4), 1248–1263.
Park, H.I., Kim, D.k., Choi, Y.-J., Pak, D., 2005. Nitrate reduction using an electrode as direct electron donor in a biofilm-electrode reactor. Process Biochem. 40 (10), 3383–3388.
Plósz, B.G., Jobbágy, A., Grady Jr., C.P.L., 2003. Factors influencing deterioration of denitrification by oxygen entering an anoxic reactor through the surface. Water Res. 37 (4), 853–863.
Popat, S.C., Ki, D., Rittmann, B.E., Torres, C.I., 2012. Importance of OH− transport from cathodes in microbial fuel cells. Chemsuschem 5 (6), 1071–1079.
Puig, S., Serra, M., Vilar-Sanz, A., Cabre, M., Baneras, L., Colprim, J., Balaguer, M.D., 2011. Autotrophic nitrite removal in the cathode of microbial fuel cells. Bioresour. Technol. 102 (6), 4462–4467.
Quince, C., Lanzen, A., Curtis, T.P., Davenport, R.J., Hall, N., Head, I.M., Read, L.F., Sloan, W.T., 2009. Accurate

determination of microbial diversity from 454 pyrosequencing data. Nat. Methods 6 (9), 639–641.
Quince, C., Lanzen, A., Davenport, R.J., Turnbaugh, P.J., 2011. Removing noise from pyrosequenced amplicons. BMC Bioinform. 12, 38.
Rabaey, K., Rozendal, R.A., 2010. Microbial electrosynthesis – revisiting the electrical route for microbial production. Nat. Rev. Microbiol. 8 (10), 706–716.
Rabaey, K., Verstraete, W., 2005. Microbial fuel cells: novel biotechnology for energy generation. Trends Biotechnol. 23 (6), 291–298.
Scherson, Y.D., Wells, G.F., Woo, S.-G., Lee, J., Park, J., Cantwell, B.J., Criddle, C.S., 2013. Nitrogen removal with energy recovery through N_2O decomposition. Energy Environ. Sci. 6 (1), 241–248.
Schloss, P.D., Westcott, S.L., Ryabin, T., Hall, J.R., Hartmann, M., Hollister, E.B., Lesniewski, R.A., Oakley, B.B., Parks, D.H., Robinson, C.J., Sahl, J.W., Stres, B., Thallinger, G.G., Van Horn, D.J., Weber, C.F., 2009. Introducing mothur: open-source, platform-independent, community-supported software for describing and comparing microbial communities. Appl. Environ. Microbiol. 75 (23), 7537–7541.
Simpson, P.J., Richardson, D.J., Codd, R., 2010. The periplasmic nitrate reductase in Shewanella: the resolution, distribution and functional implications of two NAP isoforms, NapEDABC and NapDAGHB. Microbiology 156 (Pt 2), 302–312.
Straub, K.L., Schonhuber, W.A., Buchholz-Cleven, B.E.E., Schink, B., 2004. Diversity of ferrous iron-oxidizing, nitrate-reducing bacteria and their involvement in oxygen-independent iron cycling. Geomicrobiology 21 (6), 371–378.
Sul, W.J., Cole, J.R., Jesus Eda, C., Wang, Q., Farris, R.J., Fish, J.A., Tiedje, J.M., 2011. Bacterial community comparisons by taxonomy-supervised analysis independent of sequence alignment and clustering. Proc. Natl. Acad. Sci. USA 108 (35), 14637–14642.
Virdis, B., Rabaey, K., Rozendal, R.A., Yuan, Z., Keller, J., 2010. Simultaneous nitrification, denitrification and carbon removal in microbial fuel cells. Water Res. 44 (9), 2970–2980.
Virdis, B., Rabaey, K., Yuan, Z., Keller, J., 2008. Microbial fuel cells for simultaneous carbon and nitrogen removal. Water Res. 42 (12), 3013–3024.
Vorotyntsev, V.M., Drozdov, P.N., Vorotyntsev, I.V., Smirnov, K.Y., 2009. Nitrous oxide high purification by membrane gas separation. Inorg. Mater. 45 (11), 1263–1266.
Wang, H., Qu, J., 2003. Combined bioelectrochemical and sulfur autotrophic denitrification for drinking water treatment. Water Res. 37 (15), 3767–3775.
Wang, Q., Feng, C., Zhao, Y., Hao, C., 2009. Denitrification of nitrate contaminated groundwater with a fiber-based biofilm reactor. Bioresour. Technol. 100 (7), 2223–2227.
Watanabe, T., Motoyama, H., Kuroda, M., 2001. Denitrification and neutralization treatment by direct feeding of an acidic wastewater containing copper ion and high-strength nitrate to a bio-electrochemical reactor process. Water Res. 35 (17), 4102–4110.
Weelink, S.A., Tan, N.C., ten Broeke, H., van den Kieboom, C., van Doesburg, W., Langenhoff, A.A., Gerritse, J., Junca, H., Stams, A.J., 2008. Isolation and characterization of *Alicycliphilus denitrificans* strain BC, which grows on benzene with chlorate as the electron acceptor. Appl. Environ. Microbiol. 74 (21), 6672–6681.
Wrighton, K.C., Virdis, B., Clauwaert, P., Read, S.T., Daly, R.A., Boon, N., Piceno, Y., Andersen, G.L., Coates, J.D., Rabaey, K., 2010. Bacterial community structure corresponds to performance during cathodic nitrate reduction. Isme J. 4 (11), 1443–1455.
Zhang, G., Zhao, Q., Jiao, Y., Wang, K., Lee, D.J., Ren, N., 2012. Biocathode microbial fuel cell for efficient electricity recovery from dairy manure. Biosens. Bioelectron. 31 (1), 537–543.
Zhao, Y., Feng, C., Wang, Q., Yang, Y., Zhang, Z., Sugiura, N., 2011a. Nitrate removal from groundwater by cooperating heterotrophic with autotrophic denitrification in a biofilm-electrode reactor. J. Hazard Mater. 192 (3), 1033–1039.
Zhao, Y., Feng, C., Wang, Q., Yang, Y., Zhang, Z., Sugiura, N., 2011b. Nitrate removal from groundwater by cooperating heterotrophic with autotrophic denitrification in a biofilm–electrode reactor. J. Hazard. Mater. 192 (3), 1033–1039.
Zhao, Y., Zhang, B., Feng, C., Huang, F., Zhang, P., Zhang, Z., Yang, Y., Sugiura, N., 2012. Behavior of autotrophic denitrification and heterotrophic denitrification in an intensified biofilm-electrode reactor for nitrate-contaminated drinking water treatment. Bioresour. Technol. 107 (0), 159–165.